European Journal of Nuclear Medicine and Molecular Imaging (2019) 46:437–445
https://doi.org/10.1007/s00259-018-4109-x

ORIGINAL ARTICLE

Prospective comparison of ^{18}F-FDG PET/MRI and ^{18}F-FDG PET/CT for thoracic staging of non-small cell lung cancer

Julian Kirchner[1] · Lino M. Sawicki[1] · Felix Nensa[2] · Benedikt M. Schaarschmidt[1] · Henning Reis[3] · Marc Ingenwerth[3] · Simon Bogner[4] · Clemens Aigner[5] · Christian Buchbender[1] · Lale Umutlu[2] · Gerald Antoch[1] · Ken Herrmann[6] · Philipp Heusch[1]

Received: 23 April 2018 / Accepted: 23 July 2018 / Published online: 3 August 2018

Abstract

Objectives To compare the diagnostic performance of ^{18}F-FDG PET/MRI and ^{18}F-FDG PET/CT for primary and locoregional lymph node staging in non-small cell lung cancer (NSCLC).

Methods In this prospective study, a total of 84 patients (51 men, 33 women, mean age 62.5 ± 9.1 years) with histopathologically confirmed NSCLC underwent ^{18}F-FDG PET/CT followed by ^{18}F-FDG PET/MRI in a single injection protocol. Two readers independently assessed T and N staging in separate sessions according to the seventh edition of the American Joint Committee on Cancer staging manual for ^{18}F-FDG PET/CT and ^{18}F-FDG PET/MRI, respectively. Histopathology as a reference standard was available for N staging in all 84 patients and for T staging in 39 patients. Differences in staging accuracy were assessed by McNemars chi^2 test. The maximum standardized uptake value (SUV_{max}) and longitudinal diameters of primary tumors were correlated using Pearson's coefficients.

Results T stage was categorized concordantly in ^{18}F-FDG PET/MRI and ^{18}F-FDG PET/CT in 38 of 39 (97.4%) patients. Herein, ^{18}F-FDG PET/CT and ^{18}F-FDG PET/MRI correctly determined the T stage in 92.3 and 89.7% of patients, respectively. N stage was categorized concordantly in 83 of 84 patients (98.8%). ^{18}F-FDG PET/CT correctly determined the N stage in 78 of 84 patients (92.9%), while ^{18}F-FDG PET/MRI correctly determined the N stage in 77 of 84 patients (91.7%). Differences between ^{18}F-FDG PET/CT and ^{18}F-FDG PET/MRI in T and N staging accuracy were not statistically significant ($p > 0.5$, each). Tumor size and SUV_{max} measurements derived from both imaging modalities exhibited excellent correlation ($r = 0.963$ and $r = 0.901$, respectively).

Conclusion ^{18}F-FDG PET/MRI and ^{18}F-FDG PET/CT show an equivalently high diagnostic performance for T and N staging in patients suffering from NSCLC.

Keywords PET/MRI · PET/CT · NSCLC · Thoracic staging

Julian Kirchner and Lino M. Sawicki contributed equally to this work.

✉ Julian Kirchner
Julian.Kirchner@med.uni-duesseldorf.de

[1] Department of Diagnostic and Interventional Radiology, University Dusseldorf, Medical Faculty, Moorenstrasse 5, D-40225 Dusseldorf, Germany

[2] Department of Diagnostic and Interventional Radiology and Neuroradiology, University Hospital Essen, University of Duisburg-Essen, D-45147 Essen, Germany

[3] Institute of Pathology, University Hospital Essen, West German Cancer Center, University Duisburg-Essen and the German Cancer Consortium (DKTK) Essen, D-45147 Essen, Germany

[4] Department of Medical Oncology, University Hospital Essen, West German Cancer Center, University of Duisburg-Essen, D-45122 Essen, Germany

[5] Department of Thoracic Surgery and Surgical Endoscopy, University Hospital Essen, Ruhrlandklinik, University of Duisburg-Essen, D-45147 Essen, Germany

[6] Department of Nuclear Medicine, University Hospital Essen, University of Duisburg-Essen, D-45147 Essen, Germany

Introduction

Non-small cell lung cancer (NSCLC) is the most frequently diagnosed cancer worldwide accounting for approximately 11% of total cancer diagnoses and the leading cause of cancer-related death in developed countries [1, 2]. Treatment and prognosis heavily depend on the initial cancer stage. Thus, accurate imaging-based staging of NSCLC patients plays a pivotal role for effective management and is needed to limit surgery or multimodal treatment to those patients who actually benefit from it [3]. For NSCLC patients without distant metastasis, the most important prognostic factor concerning survival is the thoracic lymph node stage [4]. ^{18}F-fluordesoxyglucose positron emission tomography/computed tomography (^{18}F-FDG PET/CT) is recommended as the first-line staging modality in potentially curable NSCLC due to its excellent diagnostic accuracy [5, 6]. Despite the high negative predictive value for detection of thoracic lymph node metastases [7, 8], ^{18}F-FDG PET/CT has a limited specificity in distinguishing inflammatory or granulomatous lymph nodes from nodal metastases [9–11]. Hence, supplementary endobronchial ultrasound-guided transbronchial needle aspiration (EBUS-TBNA) and/or esophageal ultrasonography fine-needle aspiration or cervical mediastinoscopy is suggested by current guidelines [4, 12–14]. Furthermore, staging of the primary tumor can be challenging as parenchymal changes in the postobstructive lung or tumor infiltration of the adjacent pleural and mediastinal structures can impede correct T staging in ^{18}F-FDG PET/CT [15, 16]. Compared with PET/CT, integrated PET/magnetic resonance imaging (PET/MRI) provides a higher soft-tissue contrast along with functional imaging data from diffusion-weighted imaging (DWI) and has been shown to be a valuable alternative to PET/CT for cancer staging [17, 18]. For the thoracic staging of NSCLC, a pilot study published by our group in 2014 found a similar performance of ^{18}F-FDG PET/MRI and ^{18}F-FDG PET/CT [19], but the overall evidence for ^{18}F-FDG PET/MRI in T and N staging of NSCLC is still limited and based on few small cohort studies.

Therefore, the present follow-up study aims to further validate the diagnostic performance of ^{18}F-FDG PET/MRI compared to ^{18}F-FDG PET/CT for primary and locoregional lymph node staging in a markedly larger NSCLC patient cohort.

Material & methods

Patients

This study was approved by the institutional review board (study number 11-4822-BO). After informed written consent was obtained, a total of 84 consecutive patients with histopathologically proven NSCLC (51 men, 33 women, mean age 62.5 ± 9.1 years) prospectively underwent a clinically indicated whole-body ^{18}F-FDG PET/CT subsequently followed by a thoracic ^{18}F-FDG PET/MRI. Histopathology was determined by thoracotomy (n = 49), endobronchial ultrasound biopsy (n = 27), peripheral lymph node biopsy (n = 4), or mediastinoscopy (n = 4) in every patient. Resection or biopsy specimens as the reference standard were available for N staging in all 84 patients and for T staging in 39 patients. None of the included patients received neoadjuvant therapy. The distribution of the different NSCLC subtypes is given in Table 1.

PET/CT

Whole-body ^{18}F-FDG PET/CT was performed on a Biograph mCT 128 scanner (Siemens, Healthcare GmbH, Erlangen, Germany) 60 min after intravenous injection of body weight-adapted mean activity of 275.7 ± 47.4 MBq ^{18}F-FDG. Blood glucose levels were verified to be below 150 mg/dl at injection time. After a deep-inspiration CT scan of the lungs (100 kV; automatic mA/s adjustment; slice thickness 3 mm; increment 2 mm; pitch 1), the whole-body full-dose scan was performed 70 s after 100 ml of iodinated contrast medium (Imeron 300, Bracco Imaging Deutschland GmbH, Konstanz, Germany) was intravenously administered (caudocranial scan direction from skull base to mid-thigh; 120 kV; 210 mA/s adjustment [Care Dose 4D]; slice thickness 5 mm; increment 5 mm; pitch 1). PET acquisition time was 2 min per bed position with 5–7 bed positions necessary to cover the body volume [axial field of view (FOV): 21.8 cm, matrix size 256 × 256 and a Gaussian filter of 4 mm full width at half maximum (FWHM)]. Iterative reconstruction (3 iterations and 24 subsets) was applied. PET attenuation correction was based on the whole-body CT datasets.

PET/MRI

Thoracic ^{18}F-FDG PET/MRI examinations were performed on an integrated 3-Tesla PET/MRI scanner (Biograph mMR, Siemens Healthcare GmbH, Erlangen, Germany) with a mean delay of 120 ± 16 min after ^{18}F-FDG injection. PET acquisition of the thorax was performed in one bed position for 20 min and PET images were reconstructed using the iterative ordered-subset expectation maximization algorithm, 3 iterations and 21 subsets, a Gaussian filter with 4-mm FWHM and a 344 × 344 image matrix. For MR-based attenuation correction, a two-point (fat, water) coronal 3D Dixon-VIBE sequence was performed to generate a four-compartment model (air, lungs, fat, muscle). The thoracic MRI protocol was performed according to current imaging guidelines for lung cancer [20, 21]. The following sequences were acquired using a 16-channel head/neck coil, 24-channel spine-array coil and 3 to 4 flexible 6-channel radiofrequency body array coils:

Table 1 Distribution of the different NSCLC subtypes

Subtype	n
Adenocarcinoma	59
Squamous cell carcinoma	21
Large cell carcinoma	2
Not otherwise specified NSCLC	2
Total	84

- a transversal T2-weighted (T2w) BLADE sequence in free breathing [repetition time (TR) 4360 ms; echo time (TE) 160 ms; matrix size 384; slice thickness 5 mm; field of view (FOV) 400 mm; generalized auto-calibrating partially parallel acquisition (GRAPPA) acceleration factor 2]
- a coronal T2 steady-state free-precession (TrueFISP) sequence in deep inspiration breath hold (TR 3.75 ms; TE 1.64 ms; matrix size 384; slice thickness 6 mm; FOV 330 mm; GRAPPA acceleration factor 2)
- a coronal T2 half-Fourier acquired single-shot turbo spin echo (HASTE) sequence in deep inspiration breath hold (TR 649 ms; TE 51 ms; matrix size 320; slice thickness 6 mm; FOV 330 mm; GRAPPA acceleration factor 2)
- a non-enhanced transversal T1-weighted (T1w) fast low-angle shot (FLASH) sequence in deep inspiration breath hold [TR 1510 ms; TE 2.15 ms; inversion time (TI) 1200 ms; matrix size 320; slice thickness 5 mm; FOV 400 mm; GRAPPA acceleration factor 2]
- a transversal T1w FLASH after intravenous administration of gadolinium (TR 1700 ms; TE 3.33 ms; TI 1200 ms; matrix size 256; slice thickness 7.5 mm; FOV 450 mm; GRAPPA acceleration factor 2)
- a transversal diffusion-weighted (DWI) echo-planar imaging (EPI) sequence in free breathing (TR 17,900 ms; TE 78 ms; b values: 0, 500 and 1000 s/mm^2; matrix size 160; slice thickness 5 mm; FOV 450 mm; GRAPPA acceleration factor 2)

Image analysis

The imaging datasets of the ^{18}F-FDG PET/CT and ^{18}F-FDG PET/MRI examinations were analysed independently and in random order by two readers with long-standing experience in PET/CT and PET/MRI using a dedicated OsiriX workstation (Pixmeo SARL, Bernex, Switzerland). Images were assessed in separate reading sessions with a minimum of 4 weeks apart to avoid recognition bias. The assessment of PET/CT and PET/MRI images was concordant to clinical routine by looking at the morphologic datasets (CT in PET/CT and MRI in PET/MRI) alone, corresponding PET datasets alone, as well as fused PET/CT and PET/MRI images, respectively. Staging results were then reported for the complete dataset (PET/CT and PET/MRI); no dedicated subgroup analysis was performed for morphologic or PET images alone. T and N staging was determined according to the seventh edition of the American Joint Committee on Cancer staging manual [22]. Readers were aware of patients' lung cancer diagnosis but masked to all other clinical data. Morphologic chest images (MRI and CT) as well as ^{18}F-FDG PET from PET/CT and ^{18}F-FDG PET from PET/MRI were analyzed separately and as fused PET/CT and PET/MRI datasets. In both modalities, a mass with visually increased tracer uptake within the lung parenchyma was considered as indicative of the primary tumor. Morphological signs of malignancy in lymph nodes comprised (1) increased short axis diameter, (2) central necrosis, (3) irregular shape, (4) lack of a fatty hilus sign and (5) increased contrast agent uptake [23, 24]. Region-specific size criteria were applied when assessing lymph nodes for malignancy [25, 26]. ^{18}F-FDG PET images were reviewed with and without attenuation correction to prevent false-positive findings caused by attenuation correction artefacts. The maximum standardized uptake value (SUV_{max}) was measured by placing a manually drawn region of interest over suspect lesion on attenuation-corrected PET images. Discrepant readings were resolved by consensus decision-making of both readers in a separate session.

Statistical analysis

IBM SPSS version 22 (IBM Inc., Armonk, NY, USA), R-Software environment for statistical computing (version 3.3.1, R Foundation for Statistical Computing, Vienna, Austria) and Graphpad Prism 7 (GraphPad Software, La Jolla, CA, USA) were used for statistical analysis. Descriptive analysis was performed and data are presented as mean ± SD. Correlation between ^{18}F-FDG PET/MRI and ^{18}F-FDG PET/CT was assessed using the Pearson coefficient (r) for primary tumor size and SUV_{max}. For the comparison of the primary tumor size and SUV_{max} between ^{18}F-FDG PET/CT and ^{18}F-FDG PET/MRI, a Wilcoxon signed-rank test was applied. A McNemar chi^2 test was performed to investigate whether differences in the evaluations of the correct T and N stage between ^{18}F-FDG PET/CT and ^{18}F-FDG PET/MRI were statistically significant. A p value of less than 0.05 was considered to indicate statistical significance. Furthermore, interdevice agreement between ^{18}F-FDG PET/CT and ^{18}F-FDG PET/MRI for SUV_{max} and the size of the primary tumor was analyzed using Bland–Altman plots.

Results

In the categorization of the T stage, ^{18}F-FDG PET/MRI and ^{18}F-FDG PET/CT were concordant in 38 of the 39 patients (97.4%) with resection specimens of the primary tumor as a reference standard. ^{18}F-FDG PET/MRI correctly rated the T

stage in 35 (89.7%) and ^{18}F-FDG PET/CT correctly rated the T stage in 36 (92.3%) of the 39 patients (Fig. 1). T stage was overstaged by both modalities in two identical patients. T stage was understaged in one identical patient by both modalities and in one additional patient in PET/MRI only (Fig. 2). The discrepancy in T stage in one patient was due to an underestimated lesion size of a pT2a tumor measuring 27 mm in MRI, consequently categorized falsely as T1b in ^{18}F-FDG PET/MRI, whereas the lesion was measured with 32 mm in CT and thus correctly categorized as T2a in ^{18}F-FDG PET/CT. No changes in T stage arose from additional pulmonal lesions detected by PET/CT or PET/MRI. In the categorization of the N stage, ^{18}F-FDG PET/MRI and ^{18}F-FDG PET/CT were concordant in 83 of 84 patients (98.8%). ^{18}F-FDG PET/MRI correctly rated the N stage in 77 of 84 patients (91.7%). ^{18}F-FDG PET/CT correctly rated the N stage in 78 of 84 patients (92.9%; Fig. 1). N stage was overstaged in the same patient by both hybrid imaging modalities, and in one additional patient by ^{18}F-FDG PET/MRI only. Both hybrid imaging modalities underestimated the N stage in five identical patients (6%; Fig. 3). The reason for the discrepant N stage in one patient was a moderate ^{18}F-FDG uptake seen in PET/MRI in three subcentimeter histopathologically proven benign mediastinal lymph nodes, which led to a false N2 staging of the patient in ^{18}F-FDG PET/MRI, whereas no pathologic ^{18}F-FDG uptake was seen in ^{18}F-FDG PET/CT and the patient was correctly categorized as N0 (Fig. 4). The McNemar chi^2 test yielded no significant differences between ^{18}F-FDG PET/MRI and ^{18}F-FDG PET/CT for determining the correct T stage ($p = 0.69$) and N stage ($p = 0.77$; Fig. 5).

Analysis of lesion size demonstrated that primary tumor sizes were measured slightly yet significantly smaller ($p = 0.017$) in PET/MRI (36.6 ± 19.0 mm; range: 10–91 mm) compared to PET/CT (39.1 ± 23.4 mm; range: 9–123 mm). Primary tumor size was strongly correlated between ^{18}F-FDG PET/MRI and ^{18}F-FDG PET/CT ($r = 0.963$, $p < 0.01$). A strong correlation ($r = 0.901$, $p < 0.01$) was also found for SUV_{max}. There was no statistically significant difference ($p = 0.128$) in SUV_{max} obtained from ^{18}F-FDG PET/MRI compared to ^{18}F-FDG PET/CT (12.7 ± 8.7; range: 1.5–41.6 vs. 11.7 ± 8.3; range: 1.7–36.2).

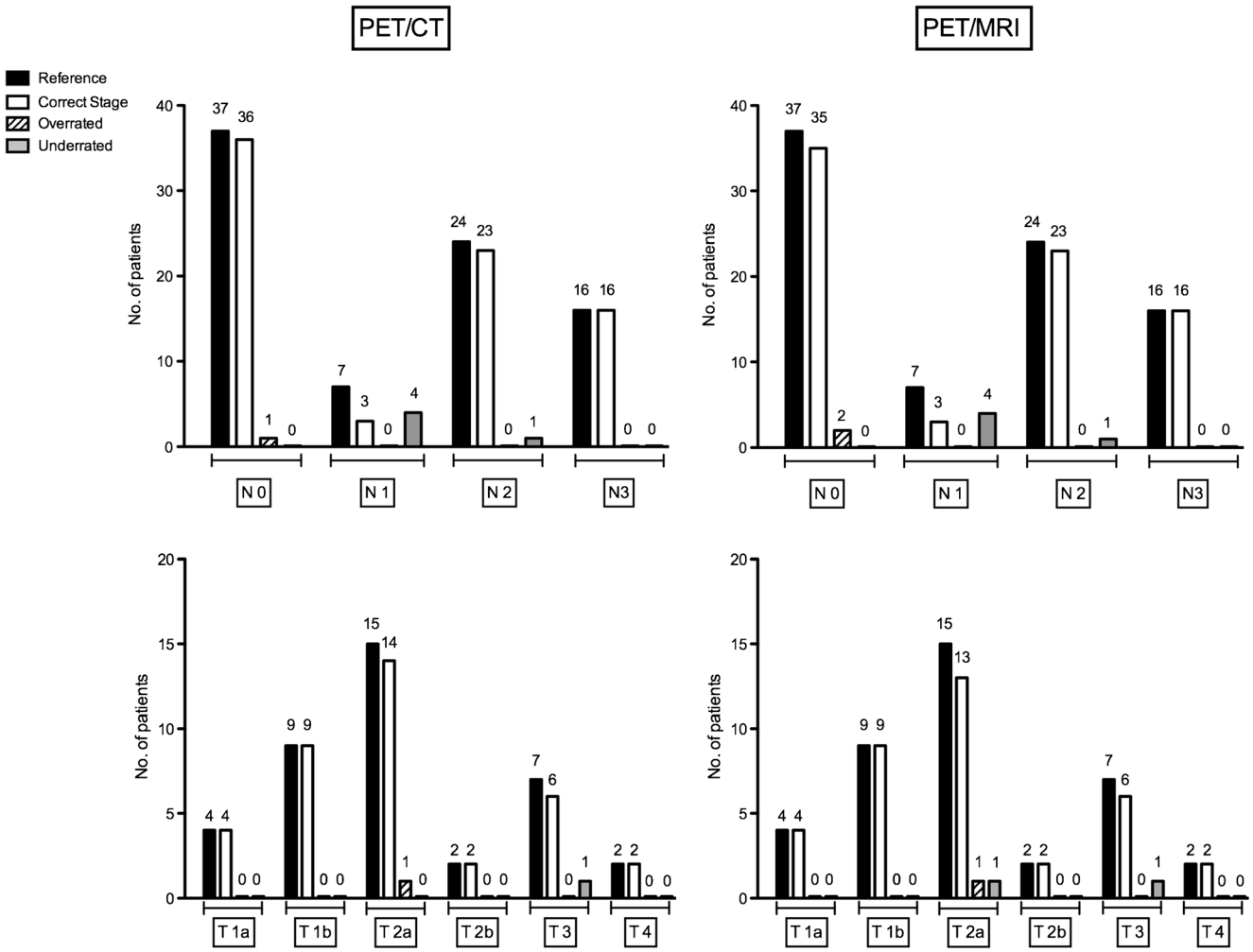

Fig. 1 Distribution of different T and N stages and corresponding ratings in PET/CT and PET/MRI

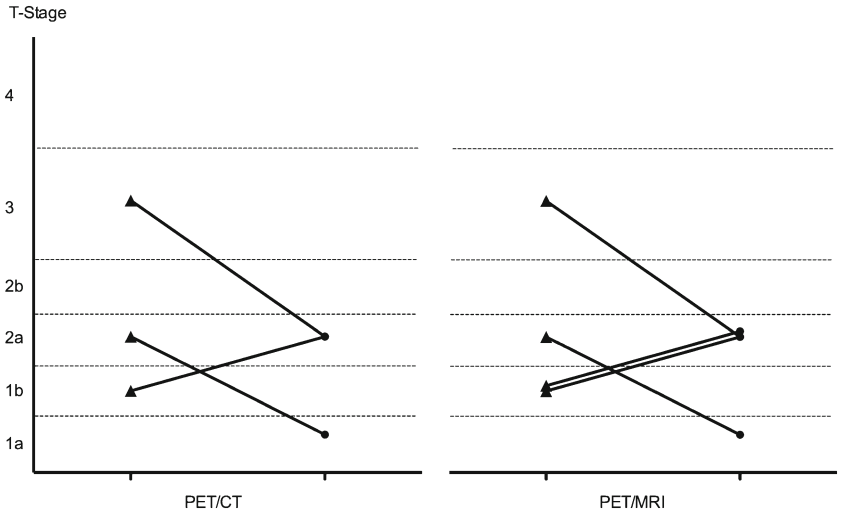

Fig. 2 Over- and understaging in T stage occurs in the same dimension in PET/CT and PET/MRI. The figure shows discrepancies in T stage classification between PET/MRI or PET/CT and the reference standard. PET/MRI and PET/CT results are marked by a triangle and the reference standard by a dot. Different T stages are separated by the dashed lines

The Bland–Altmann analysis shows the lower and upper limits of agreement between ^{18}F-FDG PET/MRI and ^{18}F-FDG PET/CT for the primary tumor size and SUV_{max} (see Figs. 6 and 7). Regression analysis revealed no systematic bias between the measurements of ^{18}F-FDG PET/MRI and ^{18}F-FDG PET/CT, but a fixed difference between the measurements.

Discussion

The present study shows the high diagnostic performance of ^{18}F-FDG PET/MRI for the thoracic staging of NSCLC and validates its non-inferiority compared to ^{18}F-FDG PET/CT as the currently recommended imaging standard. In contrast to ^{18}F-FDG PET/CT, ^{18}F-FDG PET/MRI enables whole-body NSCLC staging as a one-stop-shop examination, including the clinically required cranial MRI. As NSCLC metastases are mainly located in the brain, liver and bones, i.e. tissues where PET/MRI can be expected to yield higher detection rates, ^{18}F-FDG PET/MRI could be a useful and comprehensive tool for whole-body TNM staging [27, 28].

The cornerstone of treatment of potentially curable NSCLC is surgery, but primary resection is recommended only in stage I and II disease as well as in certain cases of stage III disease [3]. Combined with neoadjuvant chemo- and/or radiotherapy, complete operative tumor removal is frequently achieved even in advanced local disease [3]. On the other hand, patients in whom complete resection is not achievable following induction therapy are treated with individual, palliative concepts [3, 29]. Therefore, highly accurate T and N staging is mandatory as it provides necessary information on tumor burden, guides the choice of ideal treatment and determines the patients' prognosis.

Based on its slightly inferior detectability of lung lesions and vulnerability to artefacts [30, 31], PET/MRI has long been considered a merely investigational method for the staging lung cancer patients; however, recent improvements of MR techniques regarding lung nodule detection and PET/MRI's

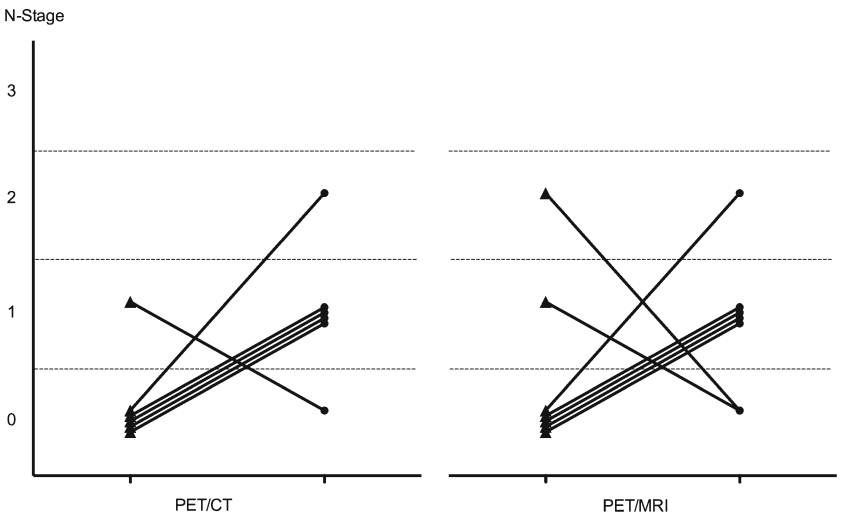

Fig. 3 Over- and understaging in N stage occurs in the same dimension in PET/CT and PET/MRI. The figure shows discrepancies in N stage classification between PET/MRI or PET/CT and the reference standard. PET/MRI and PET/CT results are marked by a triangle and the reference standard by a dot. Different N stages are separated by the dashed lines

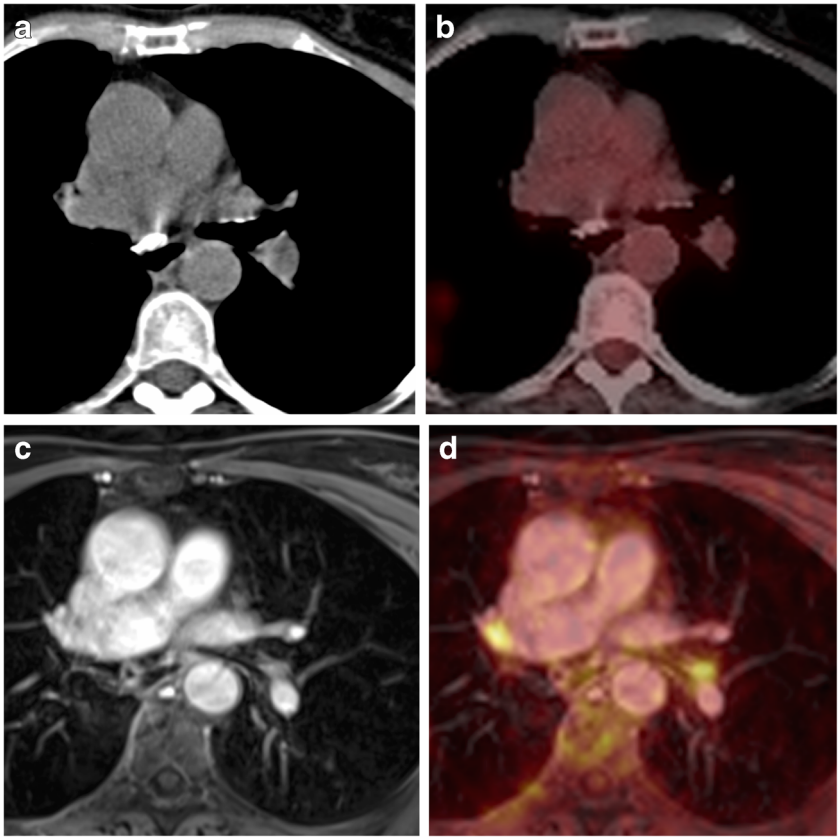

Fig. 4 Sixty-three-year-old female patient with histologically proven NSCLC in the right lung, Lymph nodes in level 4R with a short-axis diameter of 0.9 cm and at the left hilus with a short-axis diameter of 0.6 cm on a T2w HASTE MR image (**c**) and elevated FDG uptake on a fused ^{18}F-FDG PET/MR image (**d**). Identical lymph nodes of the same patient were unsuspicious on CT (**a**) and the fused ^{18}F-FDG PET/CT image (**b**). Another lymph node with identical conduct was located in level 7 (short-axis diameter 1.1 cm) in this patient. Histopathology results showed these lymph nodes as benign.

superiority in depicting mediastinal tumor invasion have sparked a renewed clinical interest [32, 33].

While contradictory results are found regarding the diagnostic accuracy of ^{18}F-FDG PET/CT vs. MRI in NSCLC staging [34–36], available data regarding the role of ^{18}F-FDG PET/MRI vs. ^{18}F-FDG PET/CT are more consistent, suggesting that both hybrid imaging are performing similarly well in NSCLC staging [19, 32, 37]. Moreover, it has been shown that both lead to identical therapeutic decisions in patients suffering from NSCLC [38]. Nevertheless, the reported results for T staging accuracy have a broad between-studies variation of 69–100%, whereas a relatively concordant rate of 80–90% is stated for N staging. In our study, we found no statistically significant difference in terms of T and N staging performance between PET/MRI and PET/CT, with a T staging accuracy of 89.7 and 92.3%, and N staging accuracy of 91.7 and 92.9% for ^{18}F-FDG PET/MRI and ^{18}F-FDG PET/CT, respectively. We also found that primary tumor sizes were measured slightly yet significantly smaller in PET/MRI compared to PET/CT conforming observations in previous studies [33]. This finding is probably due to technical differences between the two morphologic datasets. Although the higher spatial resolution of CT allows for precise lesion depiction, the fast decay of MR signal at air–tissue interfaces compromises detailed imaging at the periphery of a lesion [39]. Based on these data, our study comprises two main messages we believe to be important: First, both ^{18}F-FDG PET/CT and ^{18}F-FDG PET/MRI are well-suited and equivalent diagnostic tools for determination of the T and N stage in patients suffering from NSCLC. Second, the slightly smaller primary tumor sizes measured in ^{18}F-FDG PET/MRI are generally irrelevant for correct T staging and did not lead to significant differences compared to ^{18}F-FDG PET/CT in our study. Hence, the current results confirm the equality of PET/MRI and PET/CT reported in our pilot study [19], but the initially reported staging accuracies (100% T staging accuracy in both modalities, 90% accuracy for N stage in PET/MRI and 82% in PET/CT) are to a certain extent revised by the updated data. Huellner et al. [37] found a T staging accuracy of 69 and 81% and a N staging accuracy of 79 and 88% for PET/MRI and PET/CT, respectively. However, since they used follow-up imaging instead of histopathology as the reference standard for the majority of lesions and a shorter MRI protocol, comparability of the results is limited. In our study, T and N staging each differed in only one patient between both modalities. As ^{18}F-FDG PET/MRI examinations were performed after the clinically indicated ^{18}F-FDG PET/CT, there was a prolonged interval between tracer injection and PET acquisition in ^{18}F-FDG PET/MRI. As previously demonstrated, this may lead to a time-dependent increase of tissue ^{18}F-FDG accumulation in PET/MRI and might be the reason for the uptake of the benign mediastinal lymph nodes in one patient and differences

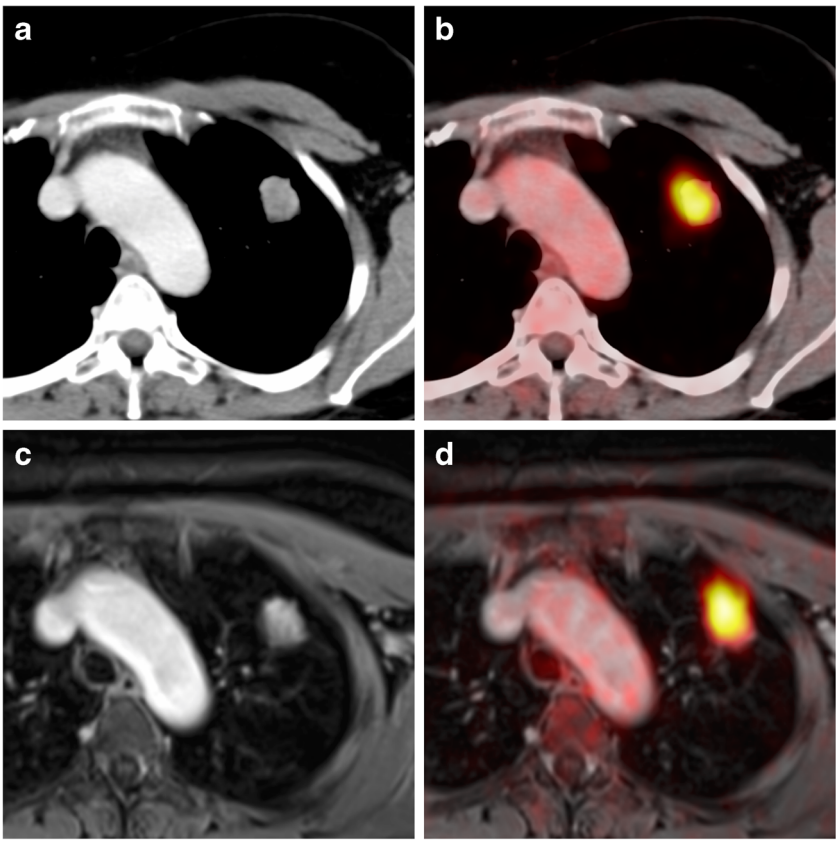

Fig. 5 ^{18}F-FDG-avid pT2a NSCLC in the left upper lobe of a 59-year-old female patient. T2w HASTE MRI (**c**), CT (**a**), fused PET/MRI (**d**) and fused PET/CT (**b**) images. The tumor measured 22 mm on MRI and 24 mm on CT. Accordingly, the primary tumor was staged correctly as T2a in both modalities

in SUV_{max} of the primary tumor [40]. The differing T staging in the other patient was due to an underestimated tumor size in ^{18}F-FDG PET/MRI. Several studies described a tendency of pulmonary lesions to be measured slightly smaller in MRI

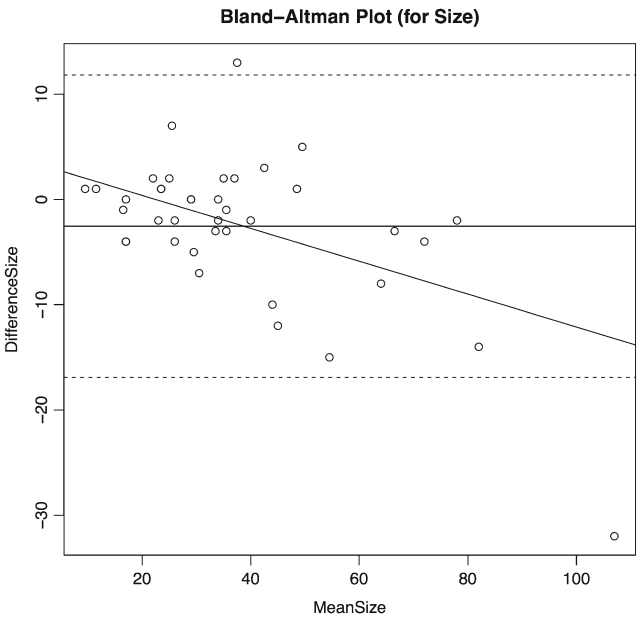

Fig. 6 Bland–Altman analysis showing lower and upper limits of agreement between ^{18}F-FDG PET/CT and ^{18}F-FDG PET/MRI for primary tumor size (in mm). The difference between primary tumor size on ^{18}F-FDG PET/MRI and ^{18}F-FDG PET/CT was plotted against their mean. The mean difference between ^{18}F-FDG PET/MRI and ^{18}F-FDG PET/CT was 2.5 mm (95% confidence interval: −16.62; +11.54). No systematic bias was revealed by regression analysis

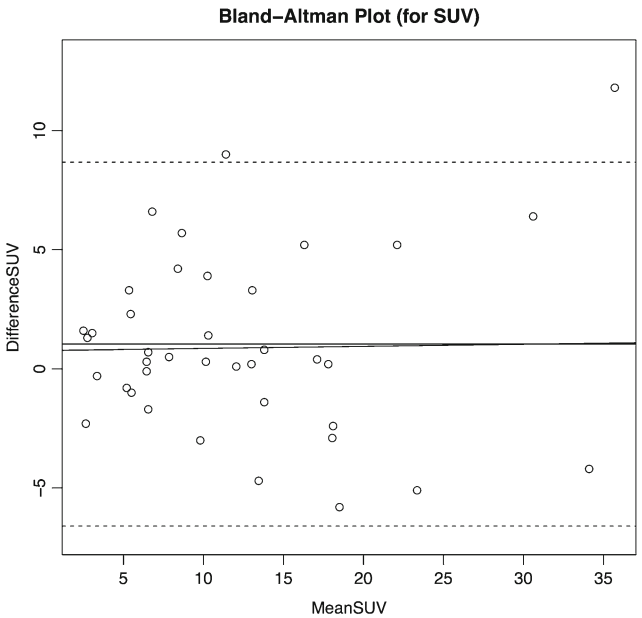

Fig. 7 Figure 5 Bland–Altman analysis showing lower and upper limits of agreement between ^{18}F-FDG PET/CT and ^{18}F-FDG PET/MRI for SUV_{max}. The difference between SUV_{max} on ^{18}F-FDG PET/MRI and ^{18}F-FDG PET/CT was plotted against their mean. The mean difference between ^{18}F-FDG PET/MRI and ^{18}F-FDG PET/CT was 1.03 (95% confidence interval: −6.44; +8.52). No systematic bias was revealed by regression analysis

than in CT [33]. However, the above-mentioned patient was the only one in whom this led to a wrong T stage assessment. Furthermore, over- and understaging occurred in the same dimension in ^{18}F-FDG PET/CT as in ^{18}F-FDG PET/MRI. Thus, there seems to be no risk of one-sided under- or overtreatment according to incorrect T and N staging with either one of the hybrid imaging modalities. Especially, no understaging in PET/MRI arose from missed pulmonal lesions compared to PET/CT.

The high comparability and strong correlation of SUV_{max} in primary tumors between ^{18}F-FDG PET/CT and ^{18}F-FDG PET/MRI is supported by results from multiple previous studies [41, 42]. Nevertheless, the above-mentioned time-dependent increase of radiotracer accumulation, differences in PET detector technology and attenuation correction are potential causes for variations in SUV_{max} between ^{18}F-FDG PET/CT and ^{18}F-FDG PET/MRI [43]. Therefore, quantitative assessment of tumor tissue, for example, in patients evaluated for response to radiation or chemotherapy should be performed on the same scanner (either PET/MRI or PET/CT) to provide reliable intraindividual measurements. Furthermore, running PET/MRI systems still comes at a markedly higher price compared to PET/CT; not only are there considerable costs of buying and maintaining the scanner, but there are also potential reimbursement issues. So far, running a PET/MR scanner in an economic manner remains challenging. Another limitation of our study was that resection specimens of primary tumors were not available in all patients. However, clinical management of NSCLC patients does not necessarily include sampling of each primary tumor.

In conclusion, the present study shows that ^{18}F-FDG PET/CT and ^{18}F-FDG PET/MRI perform equally well for T and N staging in patients suffering from NSCLC. Thus, ^{18}F-FDG PET/MRI may serve as valuable alternative to ^{18}F-FDG PET/CT for the thoracic staging of NSCLC.

Compliance with ethical standards

Conflict of interest None.

Ethical approval All procedures performed were in accordance with the ethical standards of the institutional research committee and with the principles of the 1964 Declaration of Helsinki and its later amendments.

Informed consent Informed consent was obtained from all individual participants included in the study.

References

1. Govindan R, Page N, Morgensztern D, Read W, Tierney R, Vlahiotis A, et al. Changing epidemiology of small-cell lung cancer in the United States over the last 30 years: analysis of the surveillance, epidemiologic, and end results database. J Clin Oncol. 2006;24:4539–44. https://doi.org/10.1200/JCO.2005.04.4859.
2. Torre LA, Bray F, Siegel RL, Ferlay J, Lortet-Tieulent J, Jemal A. Global cancer statistics, 2012. CA Cancer J Clin. 2015;65:87–108. https://doi.org/10.3322/caac.21262.
3. Postmus PE, Kerr KM, Oudkerk M, Senan S, Waller DA, Vansteenkiste J, et al. Early and locally advanced non-small-cell lung cancer (NSCLC): ESMO clinical practice guidelines for diagnosis, treatment and follow-up. Ann Oncol. 2017;28:iv1–iv21. https://doi.org/10.1093/annonc/mdx222.
4. De Leyn P, Dooms C, Kuzdzal J, Lardinois D, Passlick B, Rami-Porta R, et al. Revised ESTS guidelines for preoperative mediastinal lymph node staging for non-small-cell lung cancer. Eur J Cardiothorac Surg. 2014;45:787–98. https://doi.org/10.1093/ejcts/ezu028.
5. Lardinois D, Weder W, Hany TF, Kamel EM, Korom S, Seifert B, et al. Staging of non-small-cell lung cancer with integrated positron-emission tomography and computed tomography. N Engl J Med. 2003;348:2500–7. https://doi.org/10.1056/NEJMoa022136.
6. Antoch G, Stattaus J, Nemat AT, Marnitz S, Beyer T, Kuehl H, et al. Non-small cell lung cancer: dual-modality PET/CT in preoperative staging. Radiology. 2003;229:526–33. https://doi.org/10.1148/radiol.2292021598.
7. Wang J, Welch K, Wang L, Kong FM. Negative predictive value of positron emission tomography and computed tomography for stage T1-2N0 non-small-cell lung cancer: a meta-analysis. Clin Lung Cancer. 2012;13:81–9. https://doi.org/10.1016/j.cllc.2011.08.002.
8. Ambrosini V, Fanti S, Chengazi VU, Rubello D. Diagnostic accuracy of FDG PET/CT in mediastinal lymph nodes from lung cancer. Eur J Radiol. 2014;83:1301–2. https://doi.org/10.1016/j.ejrad.2014.04.035.
9. Sommer G, Wiese M, Winter L, Lenz C, Klarhofer M, Forrer F, et al. Preoperative staging of non-small-cell lung cancer: comparison of whole-body diffusion-weighted magnetic resonance imaging and 18F-fluorodeoxyglucose-positron emission tomography/computed tomography. Eur Radiol. 2012;22:2859–67. https://doi.org/10.1007/s00330-012-2542-y.
10. Roberts PF, Follette DM, von Haag D, Park JA, Valk PE, Pounds TR, et al. Factors associated with false-positive staging of lung cancer by positron emission tomography. Ann Thorac Surg. 2000;70:1154–9. discussion 9-60
11. Konishi J, Yamazaki K, Tsukamoto E, Tamaki N, Onodera Y, Otake T, et al. Mediastinal lymph node staging by FDG-PET in patients with non-small cell lung cancer: analysis of false-positive FDG-PET findings. Respiration. 2003;70:500–6.
12. Zhang R, Ying K, Shi L, Zhang L, Zhou L. Combined endobronchial and endoscopic ultrasound-guided fine needle aspiration for mediastinal lymph node staging of lung cancer: a meta-analysis. Eur J Cancer. 2013;49:1860–7. https://doi.org/10.1016/j.ejca.2013.02.008.
13. Tournoy KG, Maddens S, Gosselin R, Van Maele G, van Meerbeeck JP, Kelles A. Integrated FDG-PET/CT does not make invasive staging of the intrathoracic lymph nodes in non-small cell lung cancer redundant: a prospective study. Thorax. 2007;62:696–701. https://doi.org/10.1136/thx.2006.072959.
14. Vial MR, O'Connell OJ, Grosu HB, Hernandez M, Noor L, Casal RF, et al. Diagnostic performance of endobronchial ultrasound-guided mediastinal lymph node sampling in early stage non-small cell lung cancer: a prospective study. Respirology. 2017. https://doi.org/10.1111/resp.13162.
15. Nomori H, Watanabe K, Ohtsuka T, Naruke T, Suemasu K, Uno K. Evaluation of F-18 fluorodeoxyglucose (FDG) PET scanning for pulmonary nodules less than 3 cm in diameter, with special reference to the CT images. Lung Cancer. 2004;45:19–27. https://doi.org/10.1016/j.lungcan.2004.01.009.
16. Cheran SK, Nielsen ND, Patz EF Jr. False-negative findings for primary lung tumors on FDG positron emission tomography:

staging and prognostic implications. AJR Am J Roentgenol. 2004;182:1129–32. https://doi.org/10.2214/ajr.182.5.1821129.
17. Ehman EC, Johnson GB, Villanueva-Meyer JE, Cha S, Leynes AP, Larson PEZ, et al. PET/MRI: where might it replace PET/CT? J Magn Reson Imaging. 2017;46:1247–62. https://doi.org/10.1002/jmri.25711.
18. Spick C, Herrmann K, Czernin J. 18F-FDG PET/CT and PET/MRI perform equally well in cancer: evidence from studies on more than 2,300 patients. J Nucl Med. 2016;57:420–30. https://doi.org/10.2967/jnumed.115.158808.
19. Heusch P, Buchbender C, Kohler J, Nensa F, Gauler T, Gomez B, et al. Thoracic staging in lung cancer: prospective comparison of 18F-FDG PET/MR imaging and 18F-FDG PET/CT. J Nucl Med. 2014;55:373–8. https://doi.org/10.2967/jnumed.113.129825.
20. Kim HS, Lee KS, Ohno Y, van Beek EJ, Biederer J. PET/CT versus MRI for diagnosis, staging, and follow-up of lung cancer. J Magn Reson Imaging. 2015;42:247–60. https://doi.org/10.1002/jmri.24776.
21. Biederer J, Beer M, Hirsch W, Wild J, Fabel M, Puderbach M, et al. MRI of the lung (2/3). Why ... when ... how? Insights Imaging. 2012;3:355–71. https://doi.org/10.1007/s13244-011-0146-8.
22. Edge SB, Compton CC. The American Joint Committee on Cancer: the 7th edition of the AJCC cancer staging manual and the future of TNM. Ann Surg Oncol. 2010;17:1471–4. https://doi.org/10.1245/s10434-010-0985-4.
23. Shim SS, Lee KS, Kim BT, Chung MJ, Lee EJ, Han J, et al. Non-small cell lung cancer: prospective comparison of integrated FDG PET/CT and CT alone for preoperative staging. Radiology. 2005;236:1011–9. https://doi.org/10.1148/radiol.2363041310.
24. Kim HY, Yi CA, Lee KS, Chung MJ, Kim YK, Choi BK, et al. Nodal metastasis in non-small cell lung cancer: accuracy of 3.0-T MR imaging. Radiology. 2008;246:596–604. https://doi.org/10.1148/radiol.2461061907.
25. Ziyade S, Pinarbasili NB, Ziyade N, Akdemir OC, Sahin F, Soysal O, et al. Determination of standard number, size and weight of mediastinal lymph nodes in postmortem examinations: reflection on lung cancer surgery. J Cardiothorac Surg. 2013;8:94. https://doi.org/10.1186/1749-8090-8-94.
26. Glazer GM, Gross BH, Quint LE, Francis IR, Bookstein FL, Orringer MB. Normal mediastinal lymph nodes: number and size according to American Thoracic Society mapping. AJR Am J Roentgenol. 1985;144:261–5. https://doi.org/10.2214/ajr.144.2.261.
27. Buchbender C, Heusner TA, Lauenstein TC, Bockisch A, Antoch G. Oncologic PET/MRI, part 1: tumors of the brain, head and neck, chest, abdomen, and pelvis. J Nucl Med. 2012;53:928–38. https://doi.org/10.2967/jnumed.112.105338.
28. Buchbender C, Heusner TA, Lauenstein TC, Bockisch A, Antoch G. Oncologic PET/MRI, part 2: bone tumors, soft-tissue tumors, melanoma, and lymphoma. J Nucl Med. 2012;53:1244–52. https://doi.org/10.2967/jnumed.112.109306.
29. Novello S, Barlesi F, Califano R, Cufer T, Ekman S, Levra MG, et al. Metastatic non-small-cell lung cancer: ESMO clinical practice guidelines for diagnosis, treatment and follow-up. Ann Oncol. 2016;27:v1–v27. https://doi.org/10.1093/annonc/mdw326.
30. Sawicki LM, Grueneisen J, Buchbender C, Schaarschmidt BM, Gomez B, Ruhlmann V, et al. Evaluation of the outcome of lung nodules missed on 18F-FDG PET/MRI compared with 18F-FDG PET/CT in patients with known malignancies. J Nucl Med. 2016;57:15–20. https://doi.org/10.2967/jnumed.115.162966.
31. Sawicki LM, Grueneisen J, Buchbender C, Schaarschmidt BM, Gomez B, Ruhlmann V, et al. Comparative performance of 18F-FDG PET/MRI and 18F-FDG PET/CT regarding detection and characterization of pulmonary lesions in 121 oncologic patients. J Nucl Med. 2016. https://doi.org/10.2967/jnumed.115.167486.
32. Fraioli F, Screaton NJ, Janes SM, Win T, Menezes L, Kayani I, et al. Non-small-cell lung cancer resectability: diagnostic value of PET/MR. Eur J Nucl Med Mol Imaging. 2015;42:49–55. https://doi.org/10.1007/s00259-014-2873-9.
33. Sawicki LM, Grueneisen J, Buchbender C, Schaarschmidt BM, Gomez B, Ruhlmann V, et al. Comparative performance of 18F-FDG PET/MRI and 18F-FDG PET/CT in detection and characterization of pulmonary lesions in 121 oncologic patients. J Nucl Med. 2016;57:582–6. https://doi.org/10.2967/jnumed.115.167486.
34. Yi CA, Shin KM, Lee KS, Kim BT, Kim H, Kwon OJ, et al. Non-small cell lung cancer staging: efficacy comparison of integrated PET/CT versus 3.0-T whole-body MR imaging. Radiology. 2008;248:632–42. https://doi.org/10.1148/radiol.2482071822.
35. Plathow C, Aschoff P, Lichy MP, Eschmann S, Hehr T, Brink I, et al. Positron emission tomography/computed tomography and whole-body magnetic resonance imaging in staging of advanced nonsmall cell lung cancer–initial results. Investig Radiol. 2008;43:290–7. https://doi.org/10.1097/RLI.0b013e318163273a.
36. Ohno Y, Koyama H, Yoshikawa T, Nishio M, Aoyama N, Onishi Y, et al. N stage disease in patients with non-small cell lung cancer: efficacy of quantitative and qualitative assessment with STIR turbo spin-echo imaging, diffusion-weighted MR imaging, and fluorodeoxyglucose PET/CT. Radiology. 2011;261:605–15. https://doi.org/10.1148/radiol.11110281.
37. Huellner MW, de Galiza BF, Husmann L, Pietsch CM, Mader CE, Burger IA, et al. TNM staging of non-small cell lung cancer: comparison of PET/MR and PET/CT. J Nucl Med. 2016;57:21–6. https://doi.org/10.2967/jnumed.115.162040.
38. Schaarschmidt BM, Grueneisen J, Metzenmacher M, Gomez B, Gauler T, Roesel C, et al. Thoracic staging with 18F-FDG PET/MR in non-small cell lung cancer - does it change therapeutic decisions in comparison to 18F-FDG PET/CT? Eur Radiol. 2017;27:681–8. https://doi.org/10.1007/s00330-016-4397-0.
39. Kauczor HU, Kreitner KF. Contrast-enhanced MRI of the lung. Eur J Radiol. 2000;34:196–207.
40. Kershah S, Partovi S, Traughber BJ, Muzic RF Jr, Schluchter MD, O'Donnell JK, et al. Comparison of standardized uptake values in normal structures between PET/CT and PET/MRI in an oncology patient population. Mol Imaging Biol. 2013;15:776–85. https://doi.org/10.1007/s11307-013-0629-8.
41. Heusch P, Buchbender C, Beiderwellen K, Nensa F, Hartung-Knemeyer V, Lauenstein TC, et al. Standardized uptake values for [(1)(8)F] FDG in normal organ tissues: comparison of whole-body PET/CT and PET/MRI. Eur J Radiol. 2013;82:870–6. https://doi.org/10.1016/j.ejrad.2013.01.008.
42. Law WP, Maggacis N, Jeavons SJ, Miles KA. Concordance of 18F-FDG PET uptake in tumor and normal tissues on PET/MRI and PET/CT. Clin Nucl Med. 2017;42:180–6. https://doi.org/10.1097/RLU.0000000000001514.
43. Paulus DH, Quick HH. Hybrid positron emission tomography/magnetic resonance imaging: challenges, methods, and state of the art of hardware component attenuation correction. Investig Radiol. 2016;51:624–34. https://doi.org/10.1097/RLI.0000000000000289.